J Physiol 590.17 (2012) pp 4239–4253

The Journal of Physiology

Sequential interaction of chloride and proton ions with the fast gate steer the voltage-dependent gating in ClC-2 chloride channels

Jorge E. Sánchez-Rodríguez[1], José A. De Santiago-Castillo[2], Juan Antonio Contreras-Vite[2], Pablo G. Nieto-Delgado[1], Alejandra Castro-Chong[1] and Jorge Arreola[1]

[1] *Instituto de Física, Universidad Autónoma de San Luis Potosí, Ave. Dr Manuel Nava no. 6, San Luis Potosí, SLP 78290, México*
[2] *Instituto de Física y Matemáticas, Universidad Michoacana de San Nicolás de Hidalgo, Morelia, Mich, México*

Key points

- Plasma membrane ClC-2 chloride channels are widely distributed in our body and are important for vision and fertility.
- ClC-2 channels are gated by changes in transmembrane voltage despite of lacking a voltage sensor device. It has been hypothesized that the interaction of an external proton with the gating machinery is responsible for voltage-dependent gating.
- Here we used electrophysiological recordings and quantitative analysis under different external proton and internal chloride concentrations and found that the voltage dependence of gating is due to interaction between the passing chloride ion and the permeation pathway, with the external proton stabilizing the open state of the channel.

Abstract The interaction of either H^+ or Cl^- ions with the fast gate is the major source of voltage (V_m) dependence in ClC Cl^- channels. However, the mechanism by which these ions confer V_m dependence to the ClC-2 Cl^- channel remains unclear. By determining the V_m dependence of normalized conductance ($G_{norm}(V_m)$), an index of open probability, ClC-2 gating was studied at different $[H^+]_i$, $[H^+]_o$ and $[Cl^-]_i$. Changing $[H^+]_i$ by five orders of magnitude whilst $[Cl^-]_i/[Cl^-]_o = 140/140$ or 10/140 mM slightly shifted $G_{norm}(V_m)$ to negative V_m without altering the onset kinetics; however, channel closing was slower at acidic pH_i. A similar change in $[H^+]_o$ with $[Cl^-]_i/[Cl^-]_o = 140/140$ mM enhanced G_{norm} in a bell-shaped manner and shifted $G_{norm}(V_m)$ curves to positive V_m. Importantly, G_{norm} was >0 with $[H^+]_o = 10^{-10}$ M but channel closing was slower when $[H^+]_o$ or $[Cl^-]_i$ increased implying that ClC-2 was opened without protonation and that external H^+ and/or internal Cl^- ions stabilized the open conformation. The analysis of kinetics and steady-state properties at different $[H^+]_o$ and $[Cl^-]_i$ was carried out using a gating Scheme coupled to Cl^- permeation. Unlike previous results showing V_m-dependent protonation, our analysis revealed that fast gate protonation was V_m and Cl^- independent and the equilibrium constant for closed–open transition of unprotonated channels was facilitated by elevated $[Cl^-]_i$ in a V_m-dependent manner. Hence a V_m dependence of pore occupancy by Cl^- induces a conformational change in unprotonated closed channels, before the pore opens, and the open conformation is stabilized by Cl^- occupancy and V_m-independent protonation.

(Resubmitted 19 March 2012; accepted after revision 1 July 2012; first published online 2 July 2012)
Corresponding author J. Arreola: Instituto de Física, Universidad Autónoma de San Luis Potosí, Dr Manuel Nava no. 6, Zona Universitaria, San Luis Potosí, SLP 78290, México. Email: arreola@dec1.ifisica.uaslp.mx

DOI: 10.1113/jphysiol.2012.232660

Introduction

Opening and closing of the two independent permeation pathways in homodimeric ClC chloride channels is controlled by two fast acting gates and one slow acting gate (Miller & White, 1984; Richard & Miller, 1990; Accardi & Pusch, 2000; Zúñiga *et al.* 2004; De Santiago *et al.* 2005). Despite the lack of an intrinsic voltage sensor typically present in cation channels (Bezanilla 2008), gating in ClC channels is triggered by voltage (V_m) and is dependent on changes in $[H^+]$ and $[Cl^-]$ (Hanke & Miller, 1983; Pusch *et al.* 1995; Chen & Miller, 1996; Rychkov *et al.* 1996; Fahlke *et al.* 1997*a*; Pusch *et al.* 1999; Chen & Chen, 2001). A fast gate, also known as protopore gate, is formed by a carboxyl side chain ($–CH_2–CH_2–COO^-$) of a conserved glutamic (E) residue located in the permeation pathway (Fahlke *et al.* 1997*b*; Dutzler *et al.* 2002). Based on the structural homology of channel pores with the anion pathway structure of the EcClC Cl^-/H^+ exchanger (Dutzler *et al.* 2002), it has been proposed that in the closed state the side chain physically occludes the permeation pathway by protruding into the channel pore whilst in the open state the side chain lines the pore snorkelling toward the extracellular side. Accordingly, mutating E166 in ClC-0, E232 in ClC-1 and E207 or E213 in ClC-2 removes fast gating and also the sensitivity of gating to Cl^- and H^+ ions (Dutzler *et al.* 2003; Estévez *et al.* 2003; Niemeyer *et al.* 2003; Zúñiga *et al.* 2004; De Santiago *et al.* 2005). These observations indicate that opening of the fast gate is an essential step in ClC Cl^- channel gating and this process is dependent on both Cl^- and H^+ ions. However, the underlying mechanism by which H^+ and Cl^- ions contribute to gating appears to be slightly different in each channel despite their structural similarities.

In ClC-0 (the prototype ClC Cl^- channel amenable to single channel analysis and probably the best understood channel), extracellular acidic pH enhanced the minimal open probability at negative voltage in a V_m-independent manner, resulting in a single channel open probability of nearly 1 at all voltages without altering the single channel current (Chen & Chen, 2001). Similar results were seen with ClC-1 (Rychkov *et al.* 1996). In contrast, intracellular acidic pH shifted to more negative voltages the activation curve yielding V_m-dependent gating (Traverso *et al.* 2006; Zifarelli *et al.* 2008). Furthermore, it has been proposed that H^+ from either side of the membrane must induce slow gate opening and cross the membrane to be able to gate ClC-0 (Lisal & Maduke, 2008, but see Picollo & Pusch, 2005). However, the widely expressed ClC-2 (Thiemann *et al.* 1992) has a complex response to variations in extracellular proton concentration ($[H^+]_o$) and the effects of changes in intracellular protons ($[H^+]_i$) remain undetermined. Channel opening (determined by calculating conductance, G_{norm}) steadily increases with $[H^+]_o$ increments in the low range; however, G_{norm} decreases with further $[H^+]_o$ increments (Arreola *et al.* 2002). Such behaviour is due to titration of side chains of two residues: a glutamic acid (E207 in guinea pig ClC-2 or E213 in mouse ClC-2) whose side chain forms the fast gate and histidine 513 (guinea pig ClC-2) located in one of the extracellular loops (Niemeyer *et al.* 2003, 2009), respectively. Mutating H513 in guinea pig ClC-2 channel abolished the inhibitory effect of high $[H^+]_o$ without affecting the enhancement of G_{norm} by low increments in $[H^+]_o$. Similarly, the precise role of Cl^- ions in the V_m-dependent gating is not well understood. It has been proposed that extracellular Cl^- allosterically modulate the interaction between intracellular H^+ and the fast gate in ClC-0 (Miller, 2006; Traverso *et al.* 2006; Zifarelli *et al.* 2008).

Following the hypothesis of V_m-dependent gating of ClC-0 due to protonation of the side chain of the gating glutamate by intracellular H^+ and the analysis of $G_{norm}([H^+]_o)$ curves at different V_m in H513 ClC-2 mutant channel, a hypothesis for V_m-dependent gating of ClC-2 based on V_m-dependent titration of the side chain of the gating glutamate by extracellular H^+ was proposed (Niemeyer *et al.* 2009). In this hypothesis, intracellular Cl^- would allosterically modulate the protonation reaction. If the fast gate is within the electrical field, the open probability is strictly dependent on $[H^+]$ and the closing rate must be independent of $[H^+]$. However, if the gate is within the electrical field then either extracellular H^+ or intracellular Cl^- ions can be potentially responsible for V_m-dependent gating of ClC-2 and hence the mechanism by which intracellular Cl^- ions contribute to ClC-2 gating should be thoroughly analysed. Interestingly, in ClC-Ka and ClC-Kb, the kidney Cl^- channels that lack fast gate, high $[H^+]_o$ also abolished Cl^- current (Gradogna *et al.* 2010). A homologous histidine is present in all ClC channels in a highly conserved region located between transmembrane segments P and Q. But mutating this residue renders ClC-Ka non-functional (Gradogna *et al.* 2010) without altering the gating behaviour and Zn^{2+} sensitivity in ClC-1 (Kürz *et al.* 1999). Recently, we showed that exposing mouse ClC-2 to increasing $[Cl^-]_i$ facilitated the V_m-dependent activation ($G_{norm}(V_m)$ curve) and slowed down the fast gate closing. These processes displayed anomalous mole-fraction behaviour in Cl^-/SCN^- mixtures indicating that multi-ion occupancy of the ClC-2 pore was important for channel gating (Sanchez-Rodriguez *et al.* 2010). Furthermore, Cl^-, Br^- and SCN^- drove gating and slowed channel closing following the same sequence $SCN^- > Br^- > Cl^-$ as the sequence found for binding site occupancy in ClC-ec1 (Lobet & Dutzler, 2006; Picollo *et al.* 2009). Based on the strong homology of the anion pathway composition of ClC exchangers and channels (Estévez *et al.* 2003; Bisset *et al.* 2005; Engh *et al.* 2007) we presumed that ClC-2 has three anion binding sites (S_{int}, S_{cent} and

S_{ext}), just like the ones identified by X-ray crystallography in the ClC-ec1 Cl^-/H^+ exchanger (Dutzler *et al.* 2002, 2003). We also presumed that binding site occupancy by permeant anions was critical to ClC-2 gating. In this scenario pore occupancy and/or Cl^- movement between sites can be V_m-dependent events and thus could confer the V_m dependence, as has been proposed in ClC-0 (Engh *et al.* 2007). To gain further insights into the ClC-2 gating, in this work we reanalysed the contribution of both Cl^- and H^+ to gating. Our data analysis and modelling suggest a V_m-dependent interaction of intracellular Cl^- ions with the fast gate as the major step conferring V_m dependence to ClC-2 channels.

Methods

Cell culture, transient transfection and electrophysiological recordings

HEK cells transfected with mouse ClC-2 cDNA were cultured and used to record whole cell Cl^- current ($I_{Cl}(t)$) as previously described (De Santiago *et al.* 2005; Sanchez-Rodriguez *et al.* 2010). Briefly, $I_{Cl}(t)$ was recorded after a 5–6 min equilibration period. Step voltages (from +60 to –200 mV in 20 mV increments) delivered from the holding potential and returned to +60 mV were used to open ClC-2 channels. Throughout the experiment, the cells were maintained at 0 mV. All experiments were performed at ambient temperature (21–23°C).

Recording solutions

The standard external solution contained (in mM): TEA-Cl 139, $CaCl_2$ 0.5 and D-mannitol 100. The standard internal solution contained (in mM): TEA-Cl 140 and EGTA 20. The pH of both solutions was adjusted to 7.3 using 20 mM Hepes with TEA-OH. External and internal test solutions with different pH values were prepared by adding 20 mM of phthalate (pH 4.0 and 4.8), Mes (pH 5.5 and 6.4), Hepes (pH 7.3 and 8.2), Ampso (pH 9.1) or Caps (pH 10). Internal solutions with different $[Cl^-]$ were prepared by adding adequate amounts of TEA-Cl to obtain the desired $[Cl^-]$ without restoring ionic strength. Average tonicity, adjusted with D-mannitol, of external and internal solutions was 387.9 ± 1.9 and 347.3 ± 2.6 mosmol kg^{-1}, respectively.

Analysis

Since $[Cl^-]_i$ is critical to ClC-2 gating, we only included data with the reversal potential (V_r) near the predicted Nernst potential for Cl^- (E_{Cl}) and nearly identical G_{norm}–V_m and instantaneous tail current (I_{tail})–V_m curves (for details on this inclusion criteria see Sanchez-Rodriguez *et al.* 2010). When solutions with different $[Cl^-]$ were tested, the V_m values were corrected for junction potential errors estimated using pCLAMP (Molecular Devices, Sunnyvale, CA, USA) or series resistance errors. G_{norm} was estimated as described before (De Santiago *et al.* 2005; Sanchez-Rodriguez *et al.* 2010). Briefly, whole cell Cl^- conductance ($G = I_{Cl}/(V_m - V_r)$) were plotted as a function of V_m and fitted with a Boltzmann function to estimate maximum G. Maximum G was then used to normalize the corresponding G–V_m relationship. $G_{norm}(V_m)$ curves at different $[H^+]_i$ were obtained by normalizing each G *vs.* V_m curve against its own maximum G and then pooled. $G_{norm}(V_m)$ curves at different $[H^+]_o$ were obtained by normalizing individual G *vs.* V_m curve to its corresponding maximum G obtained under control condition $[H^+]_o = 10^{-7.3}$ M and then pooled. The resulting curves described the voltage dependence of apparent open probability ($P_A(V_m)$) in terms of normalized conductance. $G_{norm}(V_m)$ curves were fitted to a Boltzmann function (eqn (1)):

$$G_{norm} = \frac{A}{1 + e^{-\frac{zF}{RT}(V_m - V_{1/2})}} \quad (1)$$

where A is a scaling factor, z is the apparent charge, F is the Faraday constant, R is the gas constant, T is the temperature and $V_{1/2}$ is the V_m needed to reach $G_{norm} = A/2$. $I_{Cl}(t)$ values at each V_m value under different conditions ($[H^+]$ or $[Cl^-]$) were fitted with eqn (2):

$$I_{Cl}(t) = A_f\left(1 - e^{-t/\tau_f}\right) + A_s\left(1 - e^{-t/\tau_s}\right) \quad (2)$$

where A_f and A_s are the relative weights of fast and slow components and τ_f and τ_s are their corresponding time constants (De Santiago *et al.* 2005). Macroscopic closing time constants (τ_C) were calculated by fitting $G_{norm}(t)$ at +60 mV traces with eqn (3):

$$G_{norm}(t) = y_1\left(1 - e^{-t/\tau_c}\right) + y_0 \quad (3)$$

where y_0 is G_{norm} at $t = 0$ and $y_1 + y_0$ is G_{norm} in steady-state. Means ± SEM are given or plotted and the number of experiments is indicated by n.

Modelling ClC-2 gating

Different models were built using the software IonChannelLab (http://www.jadesantiago.com/Electrophysiology/IonChannelLab/) (De Santiago-Castillo *et al.* 2010). To estimate and constrain the rate constant values for each model, we performed a global fit procedure using the program IChMASCOT (http://www.jadesantiago.com/Electrophysiology/IChMASCOT/) where $I_{Cl}(t)$ and $G_{norm}(V_m)$ curves obtained at different $[H^+]_i$, different $[Cl^-]_i$ and different $[Cl^-]_o$ (from Sanchez-Rodriguez *et al.* 2010) were fitted to each model. See Supplemental

Material for details. Then IonChannelLab was used to evaluate the ability of each model and their corresponding set of rate constants to reproduce the properties of ClC-2, $I_{Cl}(t)$, $G_{norm}(V_m)$ at different $[Cl^-]_i$ and $[H^+]_o$, I_{tail}, and $V_{1/2}([Cl^-]_i, [H^+]_o)$.

Results

$[H^+]$ dependence of ClC-2 gating

Data from V_m-dependent protonation of guinea pig ClC-2 by extracellular H^+ (Niemeyer *et al.* 2009) and V_m-dependent protonation by intracellular H^+ of ClC-0 (Miller, 2006; Traverso *et al.* 2006; Zifarelli *et al.* 2008) suggest that the fast gate might be located half way through the electrical field. If so, then intracellular H^+ ions would also induce V_m-dependent gating in ClC-2. To test this possibility, experiments changing the $[H^+]_i$ from $10^{-4.0}$ to $10^{-9.1}$ M were carried out under conditions of symmetrical $[Cl^-]$ (140 mM) and constant $[H^+]_o$ ($10^{-7.3}$ M). Figure 1*A* shows whole cell Cl^- current traces ($I_{Cl}(t)$) obtained from different cells dialysed with solutions containing the indicated $[H^+]_i$ (in M) while changing the membrane potential (V_m) between +40 and –160 mV in increments of 40 mV. The onset of $I_{Cl}(t)$ appeared to be similar when $[H^+]_i$ was between $10^{-5.5}$ and $10^{-9.1}$ M, but it became slower at $[H^+]_i$ $10^{-4.0}$ M. This is summarized in Fig. 1*B* where the fast (open circles) and slow (open squares) time constants for currents measured at –120 mV are plotted as a function of $[H^+]_i$. In contrast, the time constant of closing (τ_c) at +60 mV (Fig. 1*C*) and the absolute amplitude of whole cell current (Fig. 1*D*) decreased as $[H^+]_i$ increased.

To determine the effects of $[H^+]_i$ on the V_m dependence of apparent open probability (measured as normalized conductance, G_{norm}) we constructed $G_{norm}(V_m)$ curves at each $[H^+]_i$ while $[Cl^-]_o = [Cl^-]_i = 140$ mM (Fig. 2*A*). The shape of these curves was quite similar, but their position shifted along the V_m axis as $[H^+]_i$ increased. Since varying $[H^+]_i$ has little effect on the onset kinetics, a double pulse protocol was used to determine the V_m dependence of the open probability of the fast gate P_P (De Santiago *et al.* 2005) in order to assay its H^+ dependence. As with $G_{norm}(V_m)$, the position of $P_P(V_m)$ curves on the V_m axis varied as $[H^+]_i$ increased (Fig. 2*B*). Data in Fig. 2*A* and *B* were fitted with Boltzmann eqn (1) (continuous lines) to determine the V_m needed to reach 50% of G_{norm} or P_P ($V_{1/2}$) and their apparent charge value (z). Figure 2*C* summarizes the effects of $[H^+]_i$ on $V_{1/2}$ of G_{norm} (filled circles) or $V_{1/2}$ of P_P (open circles) and the apparent charge (z) of G_{norm} (filled circles) and P_P (open circles). There was a shift of $V_{1/2}$ of G_{norm} curves to more negative potentials as $[H^+]_i$ increased from $10^{-9.1}$ to $10^{-5.5}$ M, but then a further increase in $[H^+]_i$ up to 10^{-4} M shifted the $V_{1/2}$ value back to a slightly less negative potential. A similar behaviour was observed for $V_{1/2}$ values for P_P at the $[H^+]_i$ tested. Also, the estimated apparent charge z for both G_{norm} and P_P was nearly constant, ~–1, at all $[H^+]_i$. We then reasoned that if intracellular H^+ ions activate ClC-2, then extracellular H^+ ions would not increase G_{norm}. This was not the case; when pH_o was decreased from 7.3 to 6.4 while keeping pH_i at 6.4 and $[Cl^-]_i = [Cl^-]_o = 140$ mM, the $G_{norm}(V_m)$ curve was shifted by +28.4 mV, a value similar to that observed when pH_i was set to 7.3 (see Fig. 3). We have previously shown that lowering $[Cl^-]_i$ to 10 mM unmasks the effect of $[Cl^-]_o$ on $G_{norm}(V_m)$ (Sanchez-Rodriguez *et al.* 2010). Hence, we wondered if keeping the apparent open probability low by lowering $[Cl^-]_i$ would favour regulation of $G_{norm}(V_m)$ by high $[H^+]_i$. However, compared to $[Cl^-]_i = 140$ mM, pH_i of 4.8 did not change the position of the $G_{norm}(V_m)$ curves

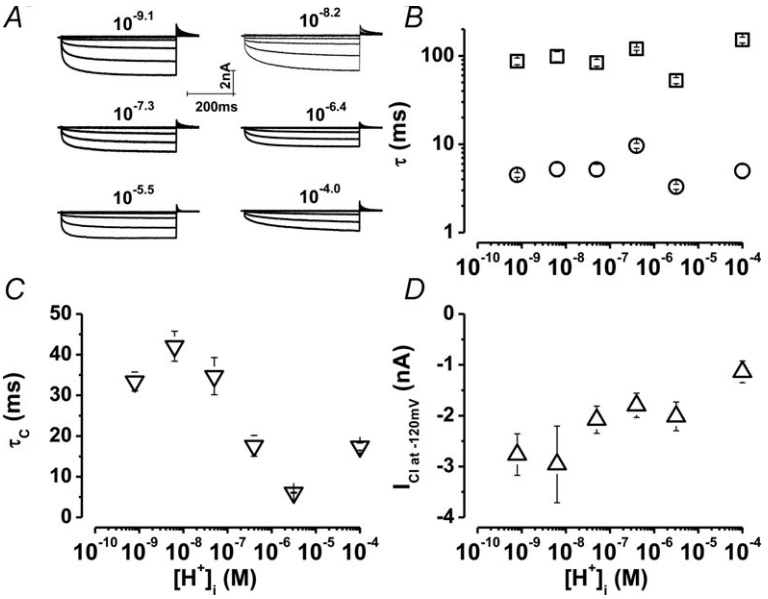

Figure 1. Regulation of I_{Cl} through ClC-2 by $[H^+]_i$
A, representative $I_{Cl}(t)$ recordings obtained from 6 different cells dialysed with internal solutions whose $[H^+]$ (in M) was adjusted to the indicated values. Currents were recorded from −160 to +40 mV, in 40 mV increments. Horizontal (200 ms) and vertical (2 nA) bars are valid for all records. $[H^+]_o = 10^{-7.3}$ M and $[Cl^-]_i = [Cl^-]_o = 140$ mM. *B*, fast (open circles) and slow (open squares) time constants as a function of $[H^+]_i$ were obtained by fitting eqn (2) to the onset phase of $I_{Cl}(t)$. *C*, time constants of closing as a function of $[H^+]_i$ were obtained by fitting eqn (3) to the offset phase of $I_{Cl}(t)$ at +60 mV. *D*, total I_{Cl} at −120 mV as a function of $[H^+]_i$. n = 5–11 different cells.

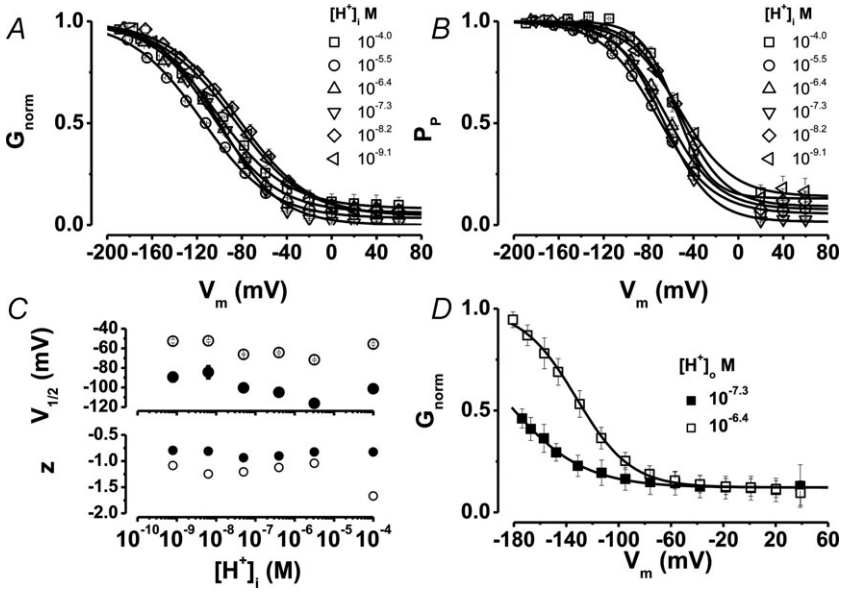

Figure 2. ClC-2 gating at different $[H^+]_i$
A, $G_{norm}(V_m)$ curves at different $[H^+]_i$. *B*, $P_P(V_m)$ curves at different $[H^+]_i$. $[H^+]_i$ (in M) and number of experiments were: $10^{-9.1}$, 9 (◁); $10^{-8.2}$, 5 (◇); $10^{-7.3}$, 11 (▽); $10^{-6.4}$, 11 (△); $10^{-5.5}$, 11 (○); $10^{-4.0}$, 7 (□). Continuous lines in *A* and *B* are fits with Boltzmann eqn (1). *C*, estimated $V_{1/2}$ and *z* values obtained by fitting with eqn (1) individual $G_{norm}(V_m)$ or $P_P(V_m)$ curves. Open symbols are parameters for $G_{norm}(V_m)$ curves while filled symbols are parameters corresponding to $P_P(V_m)$ curves. *D*, $G_{norm}(V_m)$ curves obtained from cells bathed first in a solution with pH 7.3 (filled squares) and then switched to a solution with pH 6.4 (open squares). The $[Cl^-]_i$ and pH_i were 10 mM and 6.4, respectively. $[Cl^-]_o$ was 140 mM.

when $[Cl^-]_i$ was 10 mM. $V_{1/2}$ values were –152 mV and –154 mV, with 10 mM ($n = 3$) and 140 mM ($n = 3$) $[Cl^-]_i$, respectively. In contrast, lowering pH_o from 7.3 to 6.4 with $[Cl^-]_o = 140$ mM and $[Cl^-]_i$ constant at 10 mM ($n = 3$) increased G_{norm} and shifted $G_{norm}(V_m)$ curves to the right by +29 mV (Fig. 2*D*), suggesting that high $[H^+]_i$ failed to activate ClC-2. Thus, taken together, these data show that increasing $[H^+]_i$ decreased the total current, sped up channel closing and had little effect on V_m-dependent gating of ClC-2.

In contrast to the effects of $[H^+]_i$, Fig. 3 displays the effects of increasing $[H^+]_o$ on ClC-2 gating (Arreola

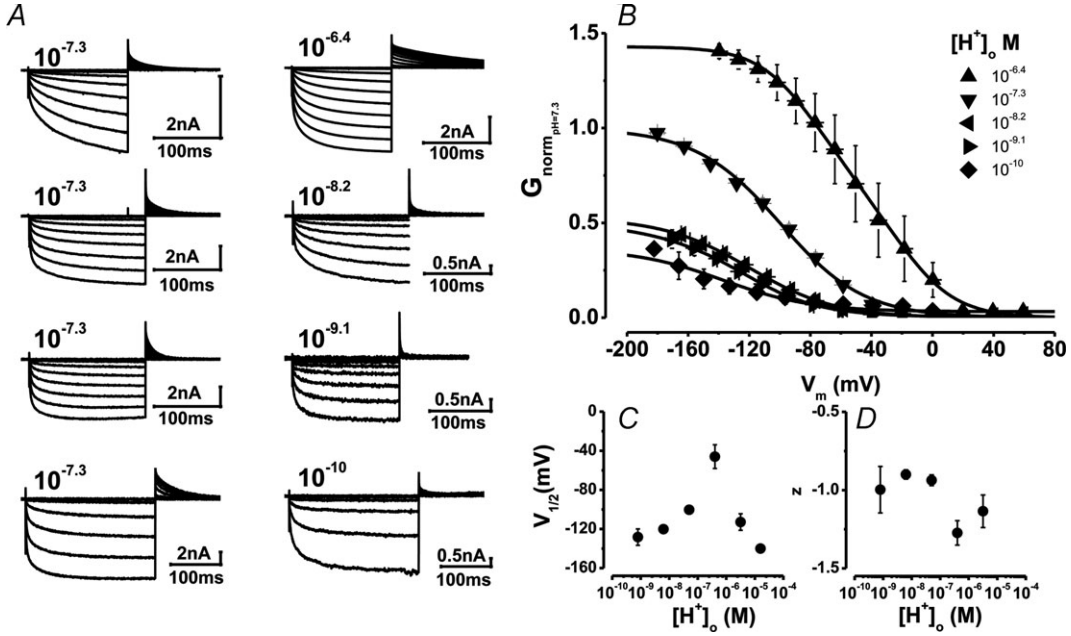

Figure 3. Effect of $[H^+]_o$ on ClC-2 gating
A, $I_{Cl}(t)$ recordings obtained from 4 different cells exposed first to control solution containing $[H^+]_o = 10^{-7.3}$ M (left traces) and then to a test solution (right traces) whose $[H^+]_o$ was adjusted to the indicated values (in M). Horizontal bars = 100 ms, valid for all recordings. Vertical bar = 2 nA is valid for control recordings and that at $10^{-6.4}$ M H^+; vertical bar = 0.5 nA is valid for all remaining recordings. pH_i 7.3 and $[Cl^-]_i = [Cl^-]_o = 140$ mM. Currents displayed were sampled at V_m: −160 to +40 mV in 20 mV increments for $10^{-6.4}$, $10^{-8.2}$ and $10^{-9.1}$ M H^+, and from −200 to +40 for 10^{-10} M H^+ in 40 mV increments. *B*, $G_{norm}(V_m)$ curves at different $[H^+]_o$ constructed using data like those shown in *A*. Continuous lines are fits with Boltzmann eqn (1) used to estimate $V_{1/2}$ and *z* values. $n = 4$ (10^{-10}, ♦),5 ($10^{-9.1}$, ▶), 5 ($10^{-8.2}$, ◀), 11 ($10^{-7.3}$, ▼), and 6 ($10^{-6.4}$, ▲). *C*, $V_{1/2}$ values at different $[H^+]_o$. *D*, *z* values at different $[H^+]_o$.

et al. 2002; Niemeyer *et al.* 2009). Figure 3*A* shows $I_{Cl}(t)$ recordings at V_m ranging from +60 to –160 mV at the indicated $[H^+]_o$. Traces on the left side are the control recordings taken at $[H^+]_o = 10^{-7.3}$ M and traces on the right side are the corresponding recordings taken from the same cell after the $[H^+]_o$ was changed. Increasing $[H^+]_o$ gradually increased I_{Cl}. Note that a sizable I_{Cl} was recorded with $[H^+]_o = 10^{-10}$ M; at –160 and –200 mV, the ratio I_{Cl} at pH 10 to I_{Cl} at pH 7.3 was 0.25 and 0.35, respectively. Supplementary Figs S1 and S2 show that a $[H^+]_o > 10^{-6.4}$ M decrease the current size. Interestingly, wild-type ClC-2 channels did not lose rectification at all $[H^+]_o$ as indicated by the decay of the tail current to 0 (Fig. 3*A*). Figure 3*B* shows $G_{norm}(V_m)$ curves at each $[H^+]_o$. In all conditions, curves show a maximum at negative V_m while at positive values G_{norm} was very close to 0 reflecting the characteristic rectification of ClC-2. Maximum G_{norm} was achieved at $[H^+]_o = 10^{-6.4}$ M and further decrements or increments in $[H^+]_o$ gradually decreased G_{norm} at all V_m (see also Supplementary Figs S1 and S2). However note that at –200 mV with $[H^+]_o = 10^{-10}$ M (filled diamonds) the G_{norm} was ~0.33 indicating that ClC-2 was opened by V_m under adverse protonation conditions. The position of $G_{norm}(V_m)$ curves on the V_m axis, measured by $V_{1/2}$ (eqn (1)), varied in a bell-shaped fashion with the $[H^+]_o$ (Fig. 3*C*). At low and high $[H^+]_o$, $V_{1/2}$ was around –140 mV but shifted to less negative V_m when the $[H^+]_o$ approached a physiological range. In contrast, z did not change with $[H^+]_o$ (Fig. 3*D*).

In addition to the effects on $G_{norm}(V_m)$ described above, increasing $[H^+]_o$ hampered ClC-2 closing indicating that external H^+ ions interacted with the fast gate. We show this by analysing the kinetics of I_{tail} recorded at +60 mV (Fig. 4) which reflects the closing of the fast gate (De Santiago *et al.* 2005) under symmetrical $[Cl^-]$ of 140 mM. Figure 4*A* shows time courses of normalized whole cell conductance (G_{norm}) at –110 and +60 mV from a cell exposed to increasing $[H^+]_o$ (green = $10^{-10.2}$ M; grey = $10^{-9.1}$ M; red = $10^{-7.3}$ M; light blue = $10^{-6.4}$ M). The analysis of $G_{norm}(t)$ using a single exponential function (dashed black lines) revealed that the opening became faster by increasing $[H^+]_o$ (Fig. 4*B*). In contrast, the G_{norm} at +60 mV reflecting the time course of channel closing was slower as $[H^+]_o$ increased (Fig. 4*C*). Overall, these observations suggest that ClC-2 is opened without protonation and the fast gate is stabilized in the open state by extracellular H^+ ions.

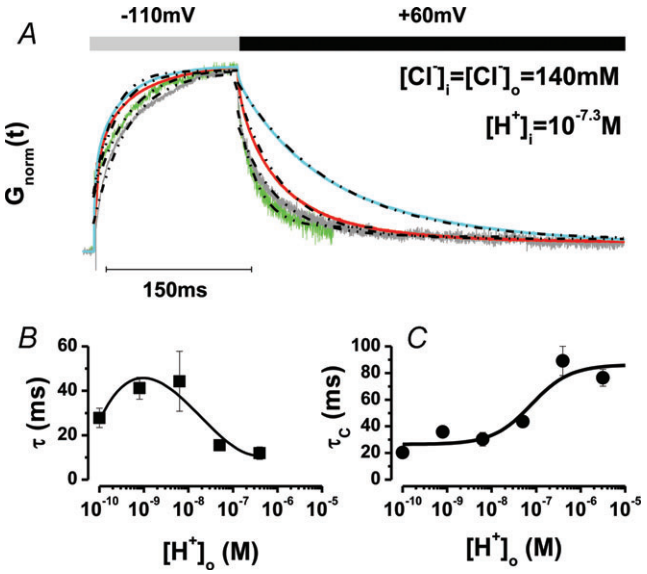

Figure 4. External H^+ ions hinder channel closing
A, time course of G_{norm} at −110 (channel opening) and +60 (channel closing) mV and at different $[H^+]_o$ ($10^{-10.2}$ M green; $10^{-9.1}$ M grey; $10^{-7.3}$ M red; $10^{-6.4}$ M light blue). Each trace is the average of four independent records. Broken lines at the top of the G_{norm} at −110 mV and +60 mV are fits with a mono-exponential function used to calculate the activation time constant (τ) or the closing time constant (τ_C) at each $[H^+]_o$. *B*, τ *vs.* $[H^+]_o$ curve. *C*, τ_C *vs.* $[H^+]_o$ curve. For each pH_o $5 < n < 9$. pH_i 7.3 and $[Cl^-]_i = [Cl^-]_o = 140$ mM.

Analysis of intracellular Cl^- and extracellular H^+ ions effects on V_m-dependent gating

For the most part ClC-2 gating was not altered by changing either $[Cl^-]_o$ (Sanchez-Rodriguez *et al.* 2010) or $[H^+]_i$, although the latter was expected to enhance gating. Since ClC-2 was opened by hyperpolarization at $[H^+]_o$ insufficient to induce protonation, we then re-evaluated the effects on V_m-dependent gating of $[Cl^-]_i$, a known facilitator of ClC-2 gating (Pusch *et al.* 1999; Sanchez-Rodriguez *et al.* 2010) at different $[H^+]_o$. Figure 5*A*–*D* displays sets of $G_{norm}(V_m)$ curves obtained from cells with $[Cl^-]_i$ fixed at 40 (Fig. 5*A*), 80 (Fig. 5*B*), 140 (Fig. 5*C*), and 200 mM (Fig. 5*D*) and bathed in external solutions whose $[H^+]_o$ was adjusted to $10^{-9.1}$ (filled inverted triangles), $10^{-8.4}$ (filled triangles), $10^{-7.3}$ (filled circles), and $10^{-6.4}$ M (filled squares). For clarity, $G_{norm}(V_m)$ curves at acidic pH_o (5.5 and 4.8) are not shown (Supplementary Fig. S1 shows curves at all pH_o). At any given V_m or $[Cl^-]_i$, G_{norm} increased when $[H^+]_o$ increased from $10^{-9.1}$ to $10^{-6.4}$ M. Although these data seem to be compatible with protonation of a binding site, S_1 (representing protonation of the fast gate which enhances G_{norm}), we find that protonation was insufficient to entirely explain these curves and those shown in Fig. 4. If ClC-2 gating is triggered solely by protonation of the fast gate ($S_1 + H_0^+ \leftrightarrow S_1^H$), then G_{norm} should be 0 when $[H^+]_o$ is low and channel closing should be independent on $[H^+]_o$. This was not the case; at any $[Cl^-]$, G_{norm} was >0 at low $[H^+]_o$ (Fig. 5*A*–*D*) and ClC-2 closing slowed down in the presence of high $[H^+]_o$ and high $[Cl^-]_i$ (Fig. 5*G*).

To gain insights into alternative mechanisms by which both H^+ and Cl^- ions drive the V_m-dependent gating of ClC-2 we took an approach identical to that applied to uncover the flip mechanism of partial agonist on ligand gated channels (Lape *et al.* 2008). Different kinetic schemes based on different putative gating mechanisms were tested for their ability to describe $I_{Cl}(t)$, $G_{norm}(V_m)$ and τ_C at different $[H^+]_o$ and $[Cl^-]_i$. We reasoned that the increased G_{norm} caused by high $[H^+]_o$ can be explained by assuming that protonation of closed channel favours the opening transitions (Supplementary Table 1). Another possibility is that protonation occurs when the channels are open and this stabilizes the open state (Schemes I and II). To quantitatively test these possibilities, two groups of kinetic Schemes were constructed based on these assumptions and a kinetic analysis was conducted.

The simplest two states kinetic scheme aimed to describe ClC-2 opening by protonation (Supplementary Table 1, row 1) gave a poor description of $[H^+]_o$ dependence of $G_{norm}(V_m)$ curves and did not predict the effect seen on the channel closing. Several variations of this scheme were also tested including those based on ideas like: protonation does not lead immediately to the open state or the channel can transit to two open states after protonation (rows 2 and 3 of Supplementary Table I). The kinetic scheme proposed by Niemeyer and co-workers (Niemeyer et al. 2009) that includes Cl^- binding was also tested (row 4). The handicap of protonation schemes is that they predicted a constant value for τ_C (Supplemental Table 1, column 3) contrary to the experimental observation (Fig. 4*C* and 5*G*).

Since the idea that protonation of closed channel could favour channel opening did not work we considered that the open state was stabilized by protonation. The simplest sequential Scheme included one closed and two open states with the protonation reaction placed in the transition $O \leftrightarrow O_H$ (Scheme I):

$$C \underset{\beta_0}{\overset{\alpha_0}{\rightleftarrows}} O \overset{K_O}{\leftrightarrow} O_H \quad \text{Scheme I}$$

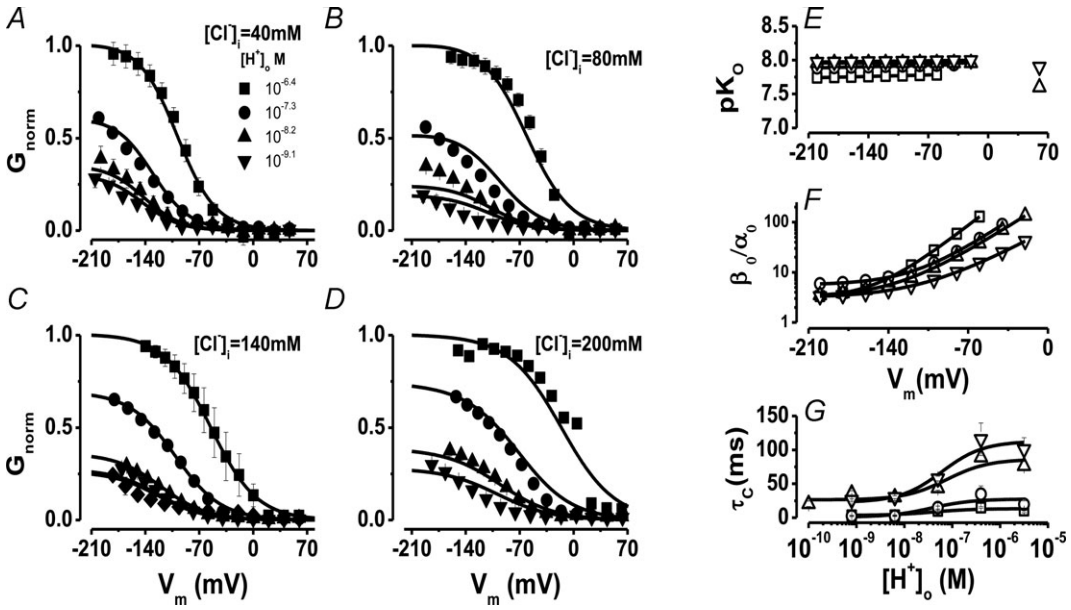

Figure 5. V_m-dependent gating of ClC-2 at different $[H^+]_o$ and $[Cl^-]_i$ ions
A, *B*, *C* and *D*, families of $G_{norm}(V_m)$ curves at different $[H^+]_o$ from cells dialysed with 40 (*A*, $5 < n < 9$), 80 (*B*, $4 < n < 10$), 140 (*C*, $4 < n < 11$) and 200 (*D*, $4 < n < 8$) mM Cl^-. $[H^+]_o$ were: $10^{-9.1}$ (▼), $10^{-8.4}$ (▲), $10^{-7.3}$ (●;), and $10^{-6.4}$ M (■). The $[H^+]_i = 10^{-7.3}$ M and $[Cl^-]_o = 140$ mM was the same in all cases. Note that G_{norm} was >0 when the $[H^+]_o$ was $10^{-9.1}$ M in all cases. Continuous lines are fits with eqn (6) (from Scheme II) used to calculate pK_O and β_0/α_0 ratio. The resulting parameters were: $[Cl^-]_i = 40$ mM: $B = 2.95$, $A = 1492$, $z = -1.02$, $pK_O = 7.8$, $z_h = -0.017$; $[Cl^-]_i = 80$ mM: $B = 5.59$, $A = 350$, $z = -0.89$, $pK_O = 7.9$, $z_h = -0.016$; $[Cl^-]_i = 140$ mM: $B = 3.2$, $A = 255$, $z = -0.83$, $pK_O = 7.96$, $z_h = 0$; $[Cl^-]_i = 200$ mM: $B = 3.1$, $A = 68.8$, $z = -0.71$, $pK_O = 8.0$, $z_h = 0.008$. SEM were similar for all V_m and for clarity only high and low $[H^+]_o$ are included. *E*, pK_O *vs.* V_m at different $[Cl^-]_i$. *F*, β_0/α_0 ratio *vs.* V_m curves for C↔O transition (Scheme II) at different $[Cl^-]_i$. Continuous lines are fits using eqn (7) with $z = -0.79$, -0.75, -0.75 and -1.13 for 40, 80, 140 and 200 mM Cl^-, respectively. *G*, τ_C *vs.* $[H^+]_o$ at different $[Cl^-]_i$. Continuous lines are fits with eqn (9). For *E*, *F* and *G* curves $[Cl^-]_i$ was (in mM): (□ = 40; ○ = 80; △ = 140, and ▽ = 200 mM). Triangles and inverted triangles plotted at +60 mV in panel *E* are pK_o values obtained from fitting eqn (9) to data shown in panel *G*.

The open probability (P_O) for channels behaving as Scheme I is given by:

$$P_{OI} = \frac{1 + \frac{[H]}{K_O}}{1 + \frac{\beta_0}{\alpha_0} + \frac{[H]}{K_O}} \quad (4)$$

To obtain the H^+, Cl^- and V_m dependence of equilibrium (K_O) and rate (α_O, β_O) constants, eqn (4) was fitted to $G_{norm}([H^+])$ curves at each $[Cl^-]_i$ and V_m. However, the off-line correction of V_m precluded construction of $G_{norm}([H^+])$ curves at each V_m. To circumvent this problem, we used the Boltzmann fits of corrected $G_{norm}(V_m)$ curves (as those shown in Fig. 3*B*) to generate corrected $G_{norm}([H^+])$ curves at each $[Cl^-]_i$ and V_m and then eqn (4) was used to fit the resulting curves (continuous lines, Supplementary Fig. S1*A*). Alternatively, the H^+ and Cl^- dependence of gating according to Scheme I can be studied by applying the Eyring rate theory (Eyring *et al.* 1949) which proposes that transition rate constants vary exponentially with V_m (see eqns (7) and (8) below). For this case, eqn (4) was fitted to $G_{norm}(V_m)$ curves obtained at pH greater than or equal to 6.4 to determine K_O, α_O and β_O (Supplementary Fig. S1*B*, continuous lines). Scheme I gave a good description of $G_{norm}([H^+]_o)$ and $G_{norm}(V_m)$ (Fig. S1*A* and *B*) and both methods used to extract the parameter values gave similar pK_0 (Supplementary Fig. S1*C*). Importantly, Scheme I predicted that the protonation constant (K_0) was V_m independent (Fig. S1*C*) while the ratio β_0/α_0 controlling the C↔O transition increased as V_m became positive (Supplementary Fig. S1*D*). For channels closing as described in Scheme I, τ_C is given by:

$$\tau_c \approx \frac{1 + \frac{[H]}{K_O}}{\beta_0} \quad (5)$$

which indicates that τ_C will linearly increase as $[H^+]_o$ increases (Supplementary Fig. S1*E*). Figures 4*C* and 5*G* show that this was not the case, at high $[H^+]_o$, τ_C levels off. The finite value of τ_C at acidic pH_o indicates that the channel can transit through the protonated open state and reach the close state, although with more difficulty. To take this into account, a protonated closed state (C_H) was added to connect the protonated open state (O_H) and the closed state (C) (Scheme II):

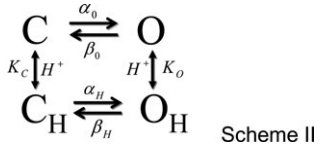

Scheme II

Scheme II is similar to that proposed by Hanke and Miller to explain the H^+ dependence of ClC-0 (Hanke & Miller, 1983). Channels behaving according to Scheme II can transit from the C (closed unprotonated) to the O (open unprotonated) state with rate constants α_0 and β_0 or from state C_H (closed protonated) to state O_H (open protonated) with rate constants α_H and β_H. Equilibrium constants for protonation of C and O states are K_C and K_O, respectively. The P_O equation for a channel gating according to Scheme II is given by:

$$P_{OII} = \frac{1 + \frac{[H^+]_o}{K_O}}{1 + \frac{[H^+]_o}{K_O} + \left(\frac{\beta_O}{\alpha_O}\right)\left(1 + \frac{[H^+]_o}{K_C}\right)} \quad (6)$$

To obtain the H^+, Cl^- and V_m dependence of equilibrium (K_O, K_C) and rate (α_O, β_O) constants for Scheme II, the same procedure above described for Scheme I was applied. First, eqn (6), without any assumption, was used to fit the corrected $G_{norm}([H^+]_o)$ (Supplementary Fig. S2*A*,) with $pK_C = 5$ since the fit did not converge or was not modified with $1 < pK_C < 5$. Second, we assumed that rate constants for C ↔ O transition and the equilibrium constant of protonation of closed channels varied exponentially with V_m and were given by eqns (7) and (8):

$$\frac{\beta_0}{\alpha_0} = A e^{-\frac{zF}{RT}V_m} + B \quad (7)$$

$$K_O = K_c/f = k_O e^{-\frac{z_h F}{RT}V_m} \quad (8)$$

where A+B is the β_0/α_0ratio at 0 mV, f is an allosteric factor to account for the protonation reaction, k_o is the equilibrium constant of protonation of open channels at 0 mV and z or z_h is the apparent charge. Then eqn (6), with V_m-dependent rate constants, was used to fit the corrected $G_{norm}(V_m)$ curves at $[H^+]_o$ up to $10^{-9.1}$ M (Supplementary Fig. S2*B*) and the results were compared to those obtained with the first approach. Supplementary Fig. S2*C* and 2*D* shows that both approaches returned nearly identical values for pK_o and the β_0/α_0 ratio, although pK_o was V_m independent while the β_0/α_0 ratio displayed V_m dependence. Since both approaches returned the same results, a full analysis of the $G_{norm}(V_m)$ at different $[H^+]_o$ and $[Cl^-]_i$ using eqn (6) was carried out to determine the H^+, Cl^- and V_m dependence of K_O, K_C, α_O and β_O (Fig. 5*A–D*, continuous lines). It is important to remark that a single set of parameters (see Fig. 5) for each $[Cl^-]_i$ tested was sufficient to fit all $G_{norm}(V_m)$ curves at such $[Cl^-]_i$. Figure 5*E* shows the pK_O values obtained using eqn (6) without any assumption (symbols) or assuming a V_m dependence on β_0/α_0 (continous lines). The equilibrium constant for the protonation reaction O↔O_H in Scheme II, was both V_m and $[Cl^-]_i$ independent with values around 7.8. Since G_{norm} was >0 at $[H^+]_o = 10^{-10}$ M and $pK_C < pK_O$ ($f = 64$ in eqn (8)), this suggested that the most likely transitions leading to the open conformation are C↔O↔O_H. In addition, given that the O↔O_H

transition is V_m and Cl^- independent, then the transition C↔O should be V_m and/or Cl^- dependent in order for ClC-2 to have V_m-dependent gating. In agreement with this idea, the β_0/α_0 ratio increased from a limiting value of ~3.5, as V_m became positive and was shifted to more positive V_m by increasing $[Cl^-]_i$ with $z = -0.79$, –0.75, –0.75, –1.13 for 40 (open squares), 80 (open circles), 140 (open triangles) and 200 (open inverted triangles) mM $[Cl^-]_i$, respectively. Overall, these data suggested that Cl^- acted on a site located within the electrical field and such interaction was responsible for V_m-dependent gating in ClC-2. Finally, for channels returning to a fully closed conformation according to Scheme II, the τ_C as a function of $[H^+]_o$ was approximated by:

$$\tau_c \approx \frac{1 + [H^+]_o / K_O}{\beta_0 + \beta_H [H^+]_o / K_O} \quad (9)$$

Unlike Scheme I, Scheme II described well the $[H^+]_0$ and $[Cl^-]_i$ dependency of the closing rate. Data in Fig. 5*G* were fitted using eqn (9) with a pK_O value of 8.5, 8.2, 7.5 and 7.7 for 40 mM (open squares), 80 mM (open circles), 140 mM (open triangles) and 200 mM (open inverted triangles) $[Cl^-]_i$, respectively. These values were plotted in Fig. 5*E* (open inverted triangles and open triangles at +60 mV) and corresponded well with those expected by extrapolating the $pK_o(V_m)$ curves to +60 mV. Taken together our findings support the hypothesis that external H^+ ions interacted with the fast gate in a V_m-independent manner and that ClC-2 remains in the open conformation for longer times when $[H^+]_o$ and $[Cl^-]_i$ are increased since both these ions hinder closing of the fast gate.

Simulating the voltage dependence of ClC2 based on gating Scheme II

Our final aim was to develop a minimal model able to reproduce the gating of mouse ClC-2. Since our data and their analysis show that permeant anions interacted with the fast gate and extracellular H^+ stabilized the open conformation, our minimal model was based on these interactions and ignored any other effects on the common gate. Models 1 and 2 based on Schemes I and II, respectively, were tested in detail to assess their ability to reproduce the kinetics and steady state properties of ClC-2 gating. To take into account the dependence of gating on the permeant Cl^- ion, it was necessary to develop coupled gating/permeation models. Given the absence of structural data for ClC-2 channels, we assumed for simplicity that the fast gate and Cl^- share the permeation pathway by presumably occupying the so-called external (S_{ext}) and central (S_{cen}) binding sites described for the ClC Cl^-/H^+ exchanger (Dutzler *et al.* 2003). Scheme III describes the occupancy by either extracellular or intracellular Cl^- (grey sphere) of an open pore (black brackets). The fast gate is represented by the black sphere and S_{cen} and S_{ext} binding sites by black circles.

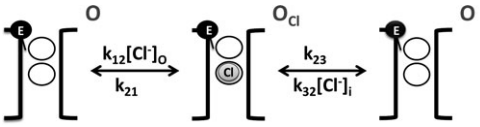

Once a Cl^- ion occupies the pore with rate constants $k_{12}[Cl^-]_o$ and $k_{32}[Cl^-]_i$, it can exit the pore with rate constants k_{21} and k_{23}. Alternatively, an intracellular Cl^- ion can occupy a closed pore with rate constants $k_3[Cl^-]_i/f$ and leave it with rate constant $k_{23}f$ as shown by Scheme IV. These rate constants are assumed to vary in an exponential manner with voltage and hence carry the voltage dependence of gating transitions.

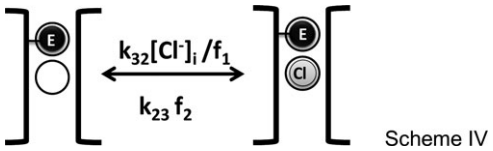

Thus, full Model 1 (Supplementary Fig. S3*A*) based on Scheme I considered transitions between empty or Cl^- occupied pores. In the closed states, the fast gate is blocking the conduction pathway. In the open states, the fast gate swings towards the extracellular side and then becomes protonated. The full open state is when a Cl^- occupies the pore and the fast gate is protonated by extracellular H^+ ($O_{Cl,H}$). Model 1 was built using the software IonChannelLab (De Santiago-Castillo *et al.* 2010) and served to perform a global fit of $I_{Cl}(t)$, $G_{norm}(V_m)$ curves and $\tau_c([H^+]_o)$ data using ICHMASCOT. The rate constants for each transition that were obtained this way were then used to simulate kinetics and steady-state properties of ClC-2. Simulations with Model 1 were able to reproduce $I_{Cl}(t)$ (Supplementary Fig. S3*B*), the $[Cl^-]_i$ and $[Cl^-]_o$ dependence of $G_{norm}(t)$ and τ_c (Supplementary Fig. S3*C* and *D*). Also, Model 1, described the $[H^+]_o$, $[Cl^-]_i$ and $[Cl^-]_o$ dependencies of $G_{norm}(V_m)$ (Supplementary Fig. S4*A*–*C*). However, as expected, the model failed to reproduce the time course of channel closing at high $[H^+]_o$ (Supplementary Fig. S5). The model failed because it does not allow transitions to the close state from the protonated states.

Model 2 assumed that (a) Cl^- interacts with the fast gate in a V_m-dependent manner according to Scheme II to facilitate the C↔O transition. The parallel shifts of P_P and G_{norm} at different $[Cl^-]_i$ (Sanchez-Rodriguez *et al.* 2010) and the modest contribution of the slow gate to ClC-2 gating (De Santiago *et al.* 2005; Yusef *et al.* 2006) support this assumption; (b) S_{ext} is near the extracellular side as suggested by the ClC-ec1 structure (Dutzler *et al.*

2003; Lisal & Maduke, 2008) and by the V_m-independent effects of extracellular H^+ and V_m-dependent effects of intracellular Cl^- on $G_{norm}(V_m)$; (c) H^+ and Cl^- regulate ClC-2 gating by hindering the fast gate closing. Figure 6*A* depicts the complete Model 2 in two levels where C and O represent closed and open states. The pore was represented by blue brackets whilst the fast gate, represented by the red sphere, was placed within the pore, closer to the extracellular side. The front level represents the gating transitions (just as Scheme II) in the absence of Cl^- whilst the back level represents the corresponding transitions after one intracellular Cl^- occupies the pore. The fast gate can be protonated by extracellular H^+ (blue sphere) and this reaction stabilizes the open conformations (O_H and $O_{Cl,H}$). Transition rate constants α and β control the C↔O transition in the absence of Cl^- and H^+. When similar transitions occurred in the presence of Cl^- (C^{Cl}↔O^{Cl}), or H^+ (C_H↔O_H), or both ($C_{Cl,H}$↔$O_{Cl,H}$), α_o and β_o rate constants are weighed by allosteric factors f_1 and f_2 or by f_H to account for the Cl^-–fast gate interaction within the pore and for the protonation state of the fast gate, respectively. $K^H{}_C$ ($= K^H{}_O \times f^2{}_H$) and $K^H{}_O$ are equilibrium constants for protonation in closed and open channels, respectively. Note that the equilibrium constant of protonation of either closed or open pores was independent of pore occupancy by Cl^-. An additional feature of Model 2 is that microscopic reversibility is maintained for cycles $C–C^{Cl}–C_H{}^{Cl}–C_H$, $C^{Cl}–O^{Cl}–O_H{}^{Cl}–C_H{}^{Cl}$, $O^{Cl}–O–O_H–O_H{}^{Cl}$, but not for cycles $C–C_{Cl}–O^{Cl}–O$ and $C_H–C_H{}^{Cl}–O_H{}^{Cl}–O_H$. A broken microscopic reversibility is expected if gating is coupled to ion permeation (Chen & Miller, 1996). $k^{Cl}{}_{C(+/-)}$ and $k^{Cl}{}_{O(+/-)}$ are rate constants controlling transitions resulting from binding (+) or unbinding (–) of one Cl^- ion to open or closed channel pore according to Schemes III and IV, respectively. These rate constants are given by:

$$k^{Cl}_{O+} = k_{12}[Cl^-]_O + k_{32}[Cl^-]_i \quad (10)$$

$$k^{Cl}_{O-} = k_{21} + k_{23} \quad (11)$$

$$k^{Cl}_{C+} = k_{32}[Cl^-]_i / f_1 \quad (12)$$

$$k^{Cl}_{C-} = k_{23} f_2 \quad (13)$$

Model 2 was built using the software IonChannelLab (De Santiago-Castillo *et al.* 2010) and then used to perform

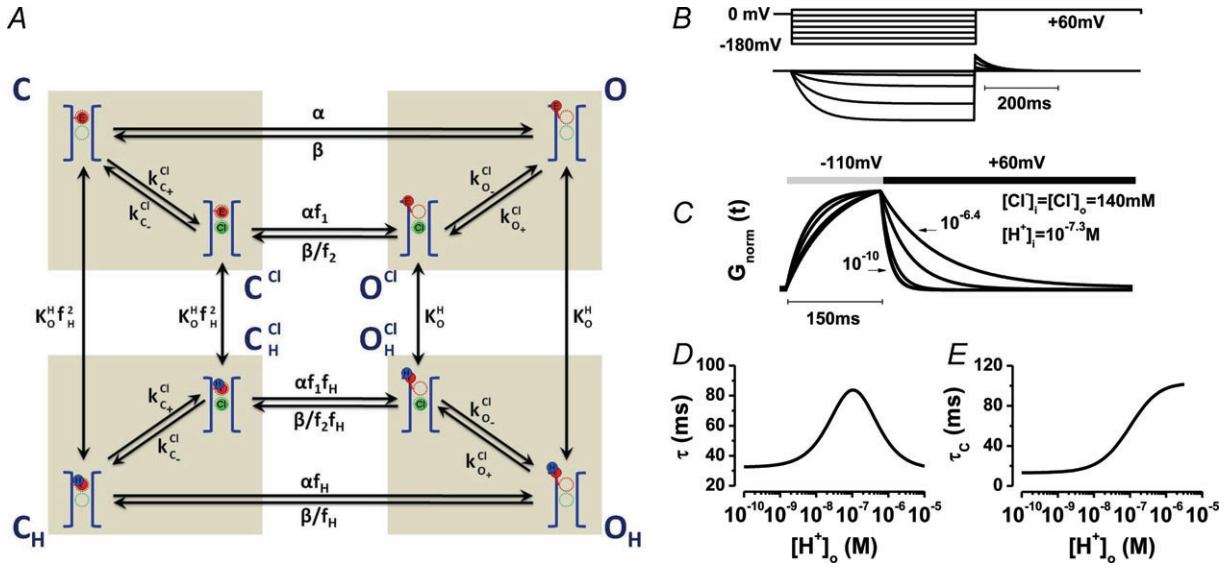

Figure 6. Model 2 for ClC-2 gating
A, kinetic model built according to Scheme II that couples movement of the fast gate to Cl^- occupancy of the pore. Rectangular boxes indicate four conformations: C = closed unprotonated, O = open unprotonated, C_H = closed protonated and O_H = open protonated. S_{cen} and S_{ext} anion binding sites are represented by dashed green and red circles, respectively. Cl^- is represented by a green sphere, H^+ by a blue sphere and the fast gate by a red sphere. Protonation of the fast gate by H^+_o is indicated by a blue sphere attach to a red sphere. Transitions between Cl^--free and Cl^--bound states are dictated by V_m-dependent rate constants. Transitions between unprotonated and protonated states are characterized by V_m-independent equilibrium constants $K_O f^2_H (= K_C)$ and K_O, respectively. Fast gate is open by electrostatic repulsion when either a Cl^- ($f_1 = 151$) or H^+ ion is bound ($f_H = 8.46$). *B*, simulated ionic currents from +60 mV to −180 mV, in 40 mV increments according to the voltage protocol shown on top. $I_{Cl}(t)$ were simulated for $[Cl^-]_i = [Cl^-]_o = 140$ mM, $pH_o = pH_i = 7.3$. *C*, simulated time course of G_{norm} at −110 and +60 with $[H^+]_o$ from $= 10^{-10}$ M to $= 10^{-6.4}$ M. *D*, opening time constant *vs.* $[H^+]_o$. *E*, closing time constant *vs.* $[H^+]_o$. Simulations were done using the parameter set listed in Table 1.

Table 1. Equilibrium constants, rate constants and allosteric parameters determined by global fitting of experimental data using Model 2

Parameter	Value or expression	Parameter	Value or expression
k_{12}	$ve^{\frac{-p_1+Vd_1F/2}{RT}}$	pK	7.9
k_{21}	$ve^{\frac{-(p_1-S_1)-Vd_1F/2}{RT}}$	α	0.06 s^{-1}
k_{23}	$ve^{\frac{-(p_2-S_1)+V(1-d_1)F/2}{RT}}$	β	229 s^{-1}
k_{32}	$ve^{\frac{-p_2-V(1-d_1)F/2}{RT}}$	f_1	151.6
p_1	10 RT	f_2	8.4
p_2	5 RT	f_H	8.46
s_1	−5 RT		
d_1	0.2		

$\nu = kT/h$, where k, T and h are the Boltzmann constant, temperature and the Planck constant, respectively. The p_i, S_i and d_i parameters represent the barrier high, well depth and fractional electrical distance from extracellular media, respectively (see Fig. 6*D*). These values or expressions were used in the simulations shown in Figs 6 and 7.

a global fit of $I_{Cl}(t)$, $G_{norm}(V_m)$ curves and $\tau_c([H^+]_o)$ data using ICHMASCOT in order to extract the rate constants for the transitions depicted in Model 2. Table 1 shows the corresponding rate constants obtained this way. These rate constants were fed into IonChannelLab (De Santiago-Castillo *et al.* 2010), to simulate ClC-2 channel kinetics and steady-state properties. Figure 6*B* shows the simulated $I_{Cl}(t)$ according to the voltage protocol depicted on top. As with real channels, simulated $I_{Cl}(t)$ displayed strong inward rectification, slow activation and large tail currents at +60 mV. The reversal potentials of simulated instantaneous current–voltage relations followed the Nernst potential for Cl^- ions, as is expected for a perfect selective channel. Model 2 also reproduced the effects of $[H^+]_o$ on the onset and offset kinetics. Figure 6*C* displays simulated G_{norm} *vs.* time traces obtained using a V_m step to −110 mV followed by step to +60 mV at different $[H^+]_o$. As with the experiment, the onset kinetics display a bell shape (Fig. 6*D*) while the offset kinetics slowed down (Fig. 6*E*) as $[H^+]_o$ increased. Furthermore, Model 2 was able to reproduce experimental data describing the effects of external $[H^+]_o$ (Fig. 7*A*), and $[Cl^-]_i$ (Fig. 7*B*) on $G_{norm}(V_m)$ curves. Importantly, when $[Cl^-]_i$ was fixed at 140 mM and $[Cl^-]_o$ was varied between 10 and 200 mM, no change was predicted on $G_{norm}(V_m)$ curves (Fig. 7*C*), just as observed experimentally (Sanchez-Rodriguez *et al.* 2010). The underlying explanation for the effects of Cl^- ions on V_m-dependent ClC-2 gating is shown in Fig. 7*D* and *E*. The probability of one intracellular Cl^- ion occupying the pore decreases as V_m becomes positive but increases as $[Cl^-]_i$ increases (Fig. 7*E*). By contrast varying $[Cl^-]_o$ between 10 and 200 mM with 140 mM $[Cl^-]_i$ does

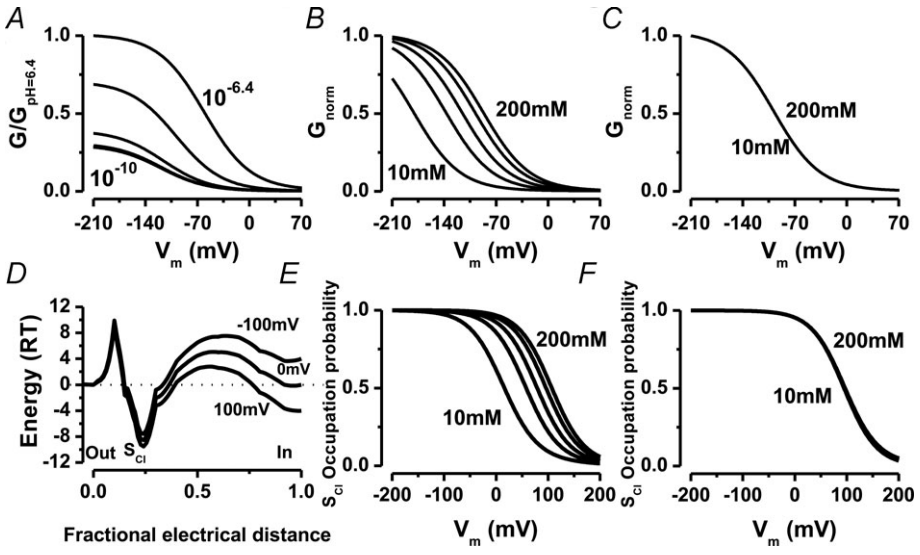

Figure 7. Simulation of steady-state properties of ClC-2 gating under different ionic conditions according to Model 2
A, $G_{norm}(V_m)$ dependence on $[H^+]_o$ (from 10^{-10} to $10^{-6.4}$ M) was simulated using Model 2. *B*, simulations of the dependence on $[Cl^-]_i$ (from 10 to 200 mM) of the $G_{norm}(V_m)$ curve. *C*, lack of effect of $[Cl^-]_o$ on $G_{norm}(V_m)$. Curves were simulated using $[Cl^-]_o$ ranging between 10 and 200 mM. *D*, energy barriers experienced by a Cl^- ion going through the permeation pathway in ClC-2 at the indicated V_m. Energy profiles were calculated considering that permeation and gating are coupled as described by Model 2. *E*, voltage dependence of probability of ClC-2 pore occupancy by Cl^- at the indicated $[Cl^-]_i$. *F*, voltage dependence of probability of ClC-2 pore occupancy by Cl^- is independent of $[Cl^-]_o$. All simulations were done using the parameter set listed in Table 1.

not alter the probability of pore occupancy (Fig. 7*F*). These distinct effects of permeant Cl^- are because an incoming Cl^- ion experience a larger energy barrier ($\sim$10 *RT*) when approaching from outside than when approaching from the inside (Fig. 7*D*). These simulations show that Model 2 reproduces most of the experimental observations regarding the H^+ and Cl^- dependence of ClC-2 gating.

Discussion

Soon after solving the structure of EcClC by X-ray diffraction (Dutzler *et al.* 2003), it was recognized that a glutamic acid residue located in the permeation pathway and its interaction with H^+ and/or Cl^- ions was fundamental for voltage gating in all ClC Cl^- channels. A large body of data show that indeed H^+ and Cl^- ions do participate in voltage gating in ClC Cl^- channels and that the side chain of a pore glutamic acid is forming the fast gate. However, the mechanism by which these ions confer voltage dependence is a matter of debate despite structural similarities among ClC channels.

We have previously shown that intracellular permeant anions contributed to mouse ClC-2 gating by interacting and then facilitating the opening of the fast gate opening (Sanchez-Rodriguez *et al.* 2010). This suggested that permeant anions play an active role in voltage gating. In the present work additional data that support the idea that Cl^- ions interact in a V_m-dependent manner with the fast gate are presented. Thus, we proposed that Cl^- is important for V_m-dependent gating in ClC-2. We observed that channel opening increased as $[H^+]_o$ increased but not when $[H^+]_i$ increased, that channel opening was larger than 0 ($G_{norm} = 0.3$) when $[H^+]_o$ was very low (10^{-10} M) and that I_{tail} kinetics which reflect closing of the fast gate became slower when $[H^+]_o$ increased. The analysis using Scheme II showed no evidence for V_m-dependent protonation of ClC-2; instead, the rate constants for a C$\leftrightarrow$O transition were sensitive to both V_m and permeant intracellular Cl^-. These later observations are contrary to what is expected (strict dependence of channel opening on $[H^+]_o$, G_{norm} almost 0 with low $[H^+]_o$ and closing kinetics independent of $[H^+]_o$) if ClC-2 gating is dictated solely by V_m-dependent protonation of the fast gate caused by *extracellular* H^+. Interestingly, the ratio β_0/α_0 for C$\leftrightarrow$O transition increased from an apparent limiting value of 3.5; this suggests that even when $[H^+]_o$ would be quite low, the channel can be opened by strong hyperpolarizations. We proposed that V_m-dependent gating is conferred by a V_m-dependent interaction between Cl^- and the fast gate with subsequent protonation by extracellular H^+ helping to stabilize the open conformation. This idea nicely unified the effects of both intracellular Cl^- and extracellular H^+ on gating and our model based on this idea reproduced the V_m-dependent gating of ClC-2.

Recently, a kinetic model for Cl^-/H^+ exchanger was proposed based on three functional states (two closed and one open) whose atomic structures were solved by x-ray crystallography (Dutzler *et al.* 2002, 2003; Feng *et al.* 2010). In that model, the binding of an intracellular H^+ to the side chain of E148 induces a displacement of the side chain towards the extracellular side and turns on the forward mode of the exchanger. In contrast, intracellular Cl^- induces the backward mode but the unprotonated E148 side chain suffers the same conformational change, a displacement towards the extracellular side. Since, ClC Cl^- channels are both structurally and functionally related to ClC Cl^-/H^+ exchangers, it is tempting to speculate that the intracellular Cl^--dependent gating of ClC-2 described in this work proceeds by a mechanism similar to that induced by intracellular Cl^- in the exchanger. In this hypothetical setting, the fast gate will be sitting on S_{ext} near the outside vestibule of ClC-2, just like suggested for ClC-0 (Bisset *et al.* 2005; Lisal & Maduke, 2008). That way, an extracellular H^+ would interact with the fast gate outside the electrical field while an intracellular Cl^- will travel nearly the entire pathway – sensing the electrical field – before reaching the fast gate. Data simulation with Model 2 indicates that pore occupancy is V_m dependent, i.e. at negative V_m the pore will be occupied by Cl^-. This will repel the fast gate and additional entry of intracellular Cl^- would further push outwardly any Cl^- ions already sitting in the pore with the consequent swing of the unprotonated fast gate toward the extracellular side. Once the gate reaches this new conformation the extracellular H^+ can bind to the gate to stabilize its open conformation. This would represent the full open/conductive state of ClC-2 and Cl^- would flow towards the extracellular space. Consequently, Cl^- will hamper closing simply because the likelihood that S_{cent} and/or S_{ext} are occupied rise as the $[Cl^-]_i$ is increased. When V_m is switched to positive values, the pore will eventually be emptied of Cl^-. Under this condition, closing of the fast gate will be dependent on dissociation of the H^+ into the extracellular space. In this way, Cl^- is able to flow without H^+ permeation (see also Picollo & Pusch, 2005) and the fast gate of ClC-2 is able to close even at high $[H^+]_o$ as experimentally observed. In summary, this gating mechanism explains how pore occupancy contributes to the V_m dependence of gating.

Although the mechanism, V_m-dependent chlorination followed by V_m-independent protonation, described by Model 2 captured most of the V_m dependence of ClC-2 gating and predicted G_{norm} *vs.* pH curves similar to those published by Niemeyer *et al.* (2009), it is still insufficient and cannot rule out for certain that external H^+ interacted with the fast gate in a V_m-dependent manner. Model 2 is an over-simplification since the effects of Cl^- and H^+

on the common gate were ignored and the anomalous mole fraction behaviour cannot be reproduced. Also, the observation that the ratio β_O/α_O cannot be described as a single exponential function of voltage – as expected for a process described by rate theory – implies that our model has some limitations, such as a limited number of transitions. An additional problem in developing sound quantitative models that help understand the gating of ClC-2 Cl^- channel is the uncertainty of the fast gate location within the pore and within the electrical field. On one hand, the structure of the ClC-ec1 Cl^-/H^+ exchanger used for homology modelling of ClC channels suggests that the physical location of the side chain of the gating glutamate would be near the outside entry of the pore (Dutzler *et al.* 2003). If this is the case, then external Cl^- and H^+ ions would affect gating in a V_m-independent manner, whilst intracellular Cl^- and H^+ ions would have to travel most of the electrical field to reach the of the side chain of the gating glutamate and in doing so, the protonation and chlorination reactions will be V_m dependent, a critical step for V_m-dependent gating. This scenario seems to be likely in ClC-0 (Chen & Chen, 2001; Traverso *et al.* 2006; Lísal & Maduke, 2008). On the other hand, theoretical analysis of EcClC structure or of the homology model for ClC-0 using Poisson–Boltzmann theory suggests that the side chain of the glutamic acid forming the fast gate may be half way within the electrical field (Faraldo-Gomez & Roux, 2004; Engh *et al.* 2007. If so, then the electrical field will alter the effective concentration of both H^+ and Cl^- around the fast gate and thus both ions could alter gating in a V_m-dependent manner. Our analysis suggests that the fast gate would be located near the extracellular side of the channel. In fact, Model 2 reproduced most of the data using an electrical distance of 0.2 for location of the fast gate. Despite of this, we cannot rule out the possibility that the gate is deeper within the electrical field. But even so, the gating process will position the fast gate near the exit side where an extracellular H^+ can bind to it. Either way, with a fast gate closer to the exit side or deep in the permeation pathway, an intracellular Cl^- ion would need to travel within the electrical field to reach the fast gate and this is essential for V_m-dependent gating in ClC-2. To conclusively demonstrate the physical location of the fast gate of ClC-2 and its interaction with H^+ and Cl^- ions, additional structural data and theoretical analysis are needed.

The present results are compatible with those we previously published using fresh dissociated rat parotid acinar cells (Arreola *et al.* 2002). For example, at –100 mV and pH 9.0, $I_{Cl,pH9.0}/I_{Cl,pH7.3}$ was 0.21 in acinar cells; in the present data G_{norm} was 0.1 with pH 9 at –100 mV and rose to nearly 0.3 at –200 mV. Although Niemeyer *et al.* (2009) reported a ratio value close to 0.5 at pH 9 and –170 mV they reached a different conclusion about V_m dependence. We wonder about possible experimental differences that may explain dissimilar conclusions. The primary sequence of mouse ClC-2 clone used in this work is quite similar (96% identity) to *Cavia porcellus* ClC-2 used by Niemeyer and co-workers. Although residues 77–86 were deleted in *C. porcellus* ClC-2, its behaviour is quite similar to the wild-type channel. Another fundamental difference is the analytical method used to extract the equilibrium constant for protonation. In our case, we considered that the channel can be opened via the unprotonated open state $O_{Cl}(C \leftrightarrow C_{Cl} \leftrightarrow O_{Cl}^H)$ or via the protonated closed state $C_H(C \leftrightarrow C_H \leftrightarrow O_{Cl}^H)$ but we make no assumption about V_m dependence on any rate constant. In addition, we took into account changes in kinetics resulting from variations in either $[Cl^-]_i$ or $[H^+]_o$. In contrast, Niemeyer *et al.* (2009) extracted the equilibrium constant of protonation from steady-state gating parameters assuming that the channel would open in a single step $(C \leftrightarrow O_{Cl}^H)$ triggered solely by protonation of the fast gate. This later case is a lump version of a more general mechanism comprising V_m-dependent and V_m-independent steps and certainly the resulting apparent equilibrium constant for protonation will be V_m dependent just because the gating is V_m dependent.

Is ClC-2 gating completely independent of $[H^+]_i$? We do not think so. $G_{norm}(V_m)$ curves shifted along the V_m axis, channel closing was sped up and total I_{Cl} decreased when pH_i was decreased. These are indications that gating is also altered by pH_i. However, all effects of pH_i were opposite to those expected for a gating facilitator. Recently, it was proposed that ClC-0 channels are opened by intracellular H^+ produced by water dissociation within the channel pore whereas the OH^- anion may occupy either S_{int} or S_{ext} sites (Zifarelli *et al.* 2008). We wonder if the effect of alkaline pH_i on ClC-2 was the result of OH^- interaction with the channel pore just like the interaction of intracellular Cl^- (Sanchez-Rodriguez *et al.* 2010). If so, then the same mechanism that explains the effects of intracellular Cl^- would explain the effects of pH_i including a positive shift of the $V_{1/2}$ parameter, a slower channel closing and current increase caused when $[OH^-]_i$ increased at alkaline pH_i.

In conclusion, we hypothesized that under physiological conditions, ClC-2 would frequently reach the full open conformation state via the unprotonated open state and that intracellular Cl^- would favour this transition by occupying the pore in a V_m-dependent manner. Extracellular H^+, on the other hand, would stabilize the open state due to a V_m-independent protonation reaction taking place after the fast gate swings towards the extracellular media. Thus, stabilization of the open state and V_m-dependent occupancy of anion binding sites will determine the open time duration and the V_m dependence of ClC-2 gating.

References

Accardi A & Pusch M (2000). Fast and slow gating relaxations in the muscle chloride channel CLC-1. *J Gen Physiol* **116**, 433–444.

Arreola J, Begenisich T & Melvin JE (2002). Conformation-dependent regulation of inward rectifier chloride channel gating by extracellular protons. *J Physiol* **541**, 103–112.

Bezanilla F (2008). How membrane proteins sense voltage. *Nat Rev Mol Cell Biol* **9**, 323–332.

Bisset D, Corry B & Chung SH (2005). The fast gating mechanism in ClC-0 channels. *Biophys J* **89**, 179–186.

Chen MF & Chen TY (2001). Different fast-gate regulation by external Cl^- and H^+ of the muscle-type ClC chloride channels. *J Gen Physiol* **118**, 23–32.

Chen TY & Miller C (1996). Nonequilibrium gating and voltage dependence of the ClC-0 Cl^- channel. *J Gen Physiol* **108**, 237–250.

De Santiago JA, Nehrke K & Arreola J (2005). Quantitative analysis of voltage-dependent gating of mouse parotid ClC-2 chloride channel. *J Gen Physiol* **126**, 591–603.

De Santiago-Castillo JA, Covarrubias M, Sánchez-Rodríguez JE, Perez-Cornejo P & Arreola J (2010). Simulating complex ion channel kinetics with IonChannelLab. *Channels* **4**, 422–428.

Dutzler R, Campbell EB, Cadene M, Chait BT & MacKinnon R (2002). X-ray structure of a ClC chloride channel at 3.0 Å reveals the molecular basis of anion selectivity. *Nature* **415**, 287–294.

Dutzler R, Campbell EB & MacKinnon R (2003). Gating the selectivity filter in ClC chloride channels. *Science* **300**, 108–112.

Engh AM, Faraldo-Gomez, JD & Maduke M (2007). The mechanism of fast-gate opening in ClC-0. *J Gen Physiol* **130**, 335–349.

Estévez R, Schroeder BC, Accardi A, Jentsch TJ & Pusch M (2003). Conservation of chloride channel structure revealed by an inhibitor binding site in ClC-1. *Neuron* **38**, 47–59.

Eyring H, Lumry R & Woodbury JW (1949). Some applications of modern rate theory to physiological systems. *Rec Chem Prog* **10**, 100–114.

Fahlke C, Durr C & George AL Jr (1997*a*). Mechanism of ion permeation in skeletal muscle chloride channels. *J Gen Physiol* **110**, 551–564.

Fahlke C, Yu HT, Beck CL, Rhodes TH & George AL Jr (1997*b*). Pore-forming segments in voltage-gated chloride channels. *Nature* **390**, 529–532.

Faraldo-Gomez JD & Roux B (2004). Electrostatics of ion stabilization in a ClC chloride channel homologue from *Escherichia coli*. *J Mol Biol* **339**, 981–1000.

Feng L, Campbell EB, Hsiung Y & Mackinnon R (2010). Structure of a eukaryotic CLC transporter defines an intermediate state in the transport cycle. *Science* **330**, 635–641.

Gradogna A, Babini E, Picollo A & Pusch M (2010). A regulatory calcium-binding site at the subunit interface of ClC-K kidney chloride channels. *J Gen Physiol* **136**, 311–323.

Hanke W & Miller C (1983). Single chloride channels from *Torpedo electroplax*. Activation by protons. *J Gen Physiol* **82**, 25–42.

Kürz LL, Klink H, Jakob I, Kuchenbecker M, Benz S, Lehmann-Horn F & Rüdel R (1999). Identification of three cysteines as targets for the Zn^{2+} blockade of the human skeletal muscle chloride channel. *J Biol Chem* **274**, 11687–11692.

Lape R, Colquhoun D & Sivilotti LG (2008). On the nature of partial agonism in the nicotinic receptor superfamily. *Nature* **454**, 722–727.

Lísal J & Maduke M (2008). The ClC-0 chloride channel is a 'broken' Cl^-/H^+ antiporter. *Nat Struct Mol Biol* **15**, 805–810.

Lobet S & Dutzler R (2006). Ion-binding properties of the ClC chloride channel selectivity filter. *EMBO J* **25**, 24–33.

Miller C & White MM (1984). Dimeric structure of single chloride channels from *Torpedo electroplax*. *Proc Natl Acad Sci U S A* **81**, 2772–2775.

Miller C (2006). ClC Chloride channels viewed through a transporter lens. *Nature* **440**, 484–489.

Niemeyer MI, Cid LP, Zúñiga L, Catalán M & Sepúlveda FV (2003). A conserved pore-lining glutamate as a voltage and chloride-dependent gate in the ClC-2 chloride channel. *J Physiol* **553**, 873–79.

Niemeyer MI, Cid LP, Yusef YR, Briones R & Sepúlveda FV (2009). Voltage-dependent and -independent titration of specific residues accounts for complex gating of a ClC chloride by extracellular protons. *J Physiol* **587**, 1387–1400.

Picollo A, Malvezzi M, Houtman JC & Accardi A (2009). Basis of substrate binding and conservation of selectivity in the CLC family of channels and transporters. *Nat Struct Mol Biol* **16**, 1294–1301.

Picollo A & Pusch M (2005). Chloride/proton antiporter activity of mammalian CLC proteins ClC-4 and ClC-5. *Nature* **436**, 420–423.

Pusch M, Jordt SE, Stein V & Jentsch TJ (1999). Chloride dependence of hyperpolarization-activated chloride channel gates. *J Physiol* **515**, 341–353.

Pusch M, Ludewig U, Rehfeldt A & Jentsch TJ (1995). Gating of the voltage dependent chloride channel ClC-0 by the permeant anion. *Nature* **373**, 527–530.

Richard EA & Miller C (1990). Steady-state coupling of ion-channel conformations to a transmembrane ion gradient. *Science* **247**, 1208–1210.

Rychkov GY, Pusch M, Astill DS, Roberts ML, Jentsch TJ & Bretag AH (1996). Concentration and pH dependence of skeletal muscle chloride channel ClC-1. *J Physiol* **497**, 423–435.

Sánchez-Rodríguez JE, De Santiago-Castillo JA & Arreola J (2010). Permeant anions contribute to voltage dependence of ClC-2 chloride channel by interacting with the protopore gate. *J Physiol* **588**, 2545–2556.

Thiemann A, Gründer S, Pusch M & Jentsch TJ (1992). A chloride channel widely expressed in epithelial and non-epithelial cells. *Nature* **356**, 57–60.

Traverso S, Zifarelli G, Aiello R & Pusch M (2006). Proton sensing of ClC-0 mutant E166D. *J Gen Physiol* **127**, 51–65.

Yusef YR, Zúñiga L, Catalán M, Niemeyer MI, Cid LP & Sepúlveda FV (2006). Removal of gating in voltage-dependent ClC-2 chloride channel by point mutations affecting the pore and C-terminus CBS-2 domain. *J Physiol* **572**, 173–181.

Zifarelli G, Murgia AR, Soliani P & Pusch M (2008). Intracellular proton regulation of ClC-0. *J Gen Physiol* **132**, 185–198.

Zúñiga L, Niemeyer MI, Varela D, Catalán M, Cid LP & Sepúlveda FV (2004). The voltage-dependent ClC-2 chloride channel has a dual gating mechanism. *J Physiol* **555**, 671–682.

Author contributions

J.E.S.R. designed research, performed research and wrote the paper. J.A.C.V. analysed and modelled data. P.G.N.D. performed research and analysed data. A.C.C. performed research and analysed data. J.A.D.S.C. designed research, analysed and modelled data and wrote the paper. J.A. designed research, analysed data and wrote the paper. All authors approved the final version for publication.

Acknowledgements

The authors thank Dr P. Pérez-Cornejo for critical comments on the manuscript and C. Y. Hernandez-Carballo for excellent technical assistance. This work was supported by grant 79897 (CONACyT, Mexico). J.E.S.R., J.A.C.V., P.G.N.D. and A.C.C. hold Fellowships from CONACyT, Mexico (166286, 35676, 192353 and 335900).

Author's present address

J. E. Sánchez-Rodríguez: Department of Biochemistry and Molecular Biology, University of Chicago.